

## **SUPPLEMENTARY MATERIALS OF:**

# **Past Analogues of Deoxygenation Events in the Mediterranean Sea: A Tool to Constrain Future Impacts**

## **1-Materials and Methods**

### **1.1 Calcareus nannofossils analysis**

Taxonomic identification follows Young et al. (2017, Nannotax3 website, <https://www.mikrotax.org/Nannotax3>). During the counting phase, two different variety of *Emiliana huxleyi* which differs in terms of degree of calcification were recognized and counted separately as *E. huxleyi* light calcified and *E. huxleyi* moderate calcified (EHLC and EHMC, respectively) following the outcomes of Crudeli et al. (2004).

### **1.2 Foraminifera analysis**

Observations were made with a stereomicroscope at 100x.

During the quantitative analysis, sinistrally and dextrally coiled specimens of *Neogloboquadrina pachyderma* were counted separately, indicated respectively with the names *Neogloboquadrina pachyderma* and *Neogloboquadrina incompta* (Darling et al., 2006). The two morphotypes of *Globigerinoides ruber* were also counted separately, as *G. ruber* var. *alba* and *G. ruber* var. *rosea*. The same distinction was applied to the pink and white morphotypes of *Globigerina rubescens* (reported as *G. rubescens* var. *rosea* e *G. rubescens* var. *alba*).

## **2-Results**

### **2.1 Radiometric age**

Depth (cm)	$^{14}\text{C}$ cal. yrs BP	$\pm$	Tephra age	Sed. rate (cm/kyr)
7.0			79 d.C.	
20.0	5794	85		2.243
26.5	8265	79		2.630
27.5	8562	110		3.367
35.5	10472	105		3.926
40.5	11490	165		4.911
65.5	19116	124		3.278
80.5	20912	148		8.351
85.5	22932	165		2.475
99.5	27656	108		2.116

Table S1:  $^{14}\text{C}$  cal. BP vs depth and the obtained sedimentation rate along with the standard deviation. The tephra age of the Z1 eruption was added as additional tie point for build the age model.

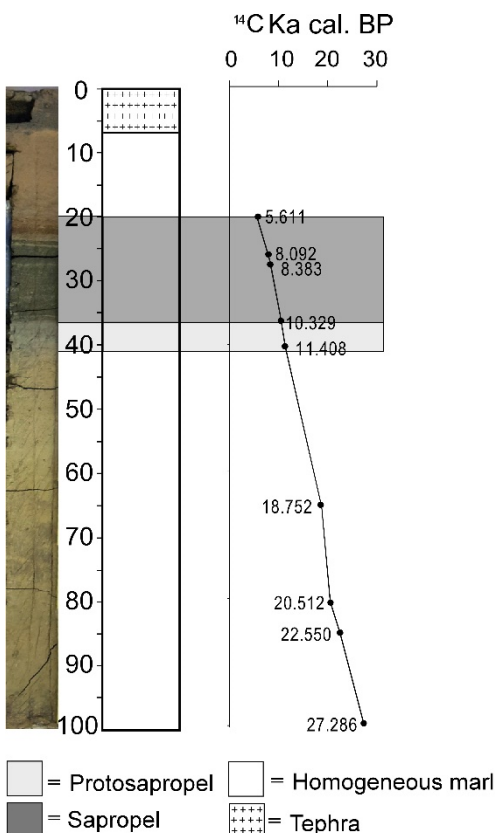


Figure S1: core M25/4-12, its schematic log and the sedimentation rate.

## 2.2 Calcareous nannofossils assemblage

Calcareous nannofossils relative abundance variation are reported in the supplementary materials.

The calcareous nannofossils assemblage consists of 20 species of coccolithophores and 1

calcareous dinoflagellate. The most abundant species is EHLC and EHMC, followed by *Florisphaera profunda*, *Rhabdosphaera spp* (*Rhabdosphaera claviger* and *Rhabdosphaera stylifer*), *Syracosphaera spp*, *Helicosphaera carteri*, *Syracosphaera sp1* and Reworked species; the rare species are *Umbilicosphaera spp*, *Scapholithus fossils*, *Coccolithus pelagicus*, *Umbellophaera spp*, *Discosphaera tubifera*; finally the extremely rare species (relative abundance lower than 1%) *Calcidiscus leptoporus*, *Thoracosphaera spp.*, *Pontosphaera multipora*, *Holococcolithus*, *Gladiolithus flabellatus*, *Calcidiscus macyntirei* and *Ceratolithus spp..*

In the lower part of the studied interval *EHMC* dominates the assemblage (from 99,5 to 80,5 cm), replaced by *EHLC* from 80,5 to 17,5 cm. At this depth *EHMC* turn to be the most abundant species; this shift is observed at the top of S1. *Florisphaera profunda* occurs throughout the core and shows increasing abundance (11.7 %) at 70.50 cm reaching high values between 39.5 cm and Cm 24.5 in the sapropel. Noteworthy two negative peaks at 35.5 and 27.5 cm.

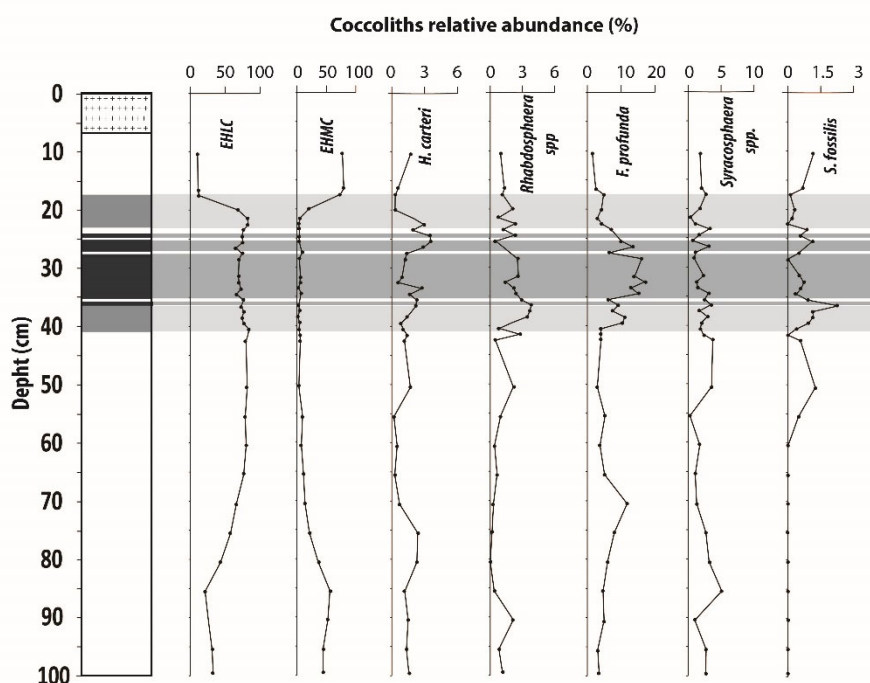


Figure S2: Calcareous nannofossil relative abundance.

## 2.3 Foraminifera

Foraminifer abundances trends are reported in the supplementary material. Planktic foraminifers are present throughout the studied interval; the assemblage was overall dominated by *Turborotalita quinqueloba*, which shows the highest abundance from 50.5 cm upward in the core. *Negloboquadrina imcopta* was rather abundant in the lower part of the core until 60.5 cm; from this level it always shows abundance less than 10%. A similar pattern was observed for *Globoratalia scitula*, which almost disappear from 55.5 cm upward in the core. *Globigerina gomitus* shows rather high abundance in the lower part of the core until it starts to significantly decreases from the top of the protosapropel layer (35.5 cm). The S1 layer is characterised by an increase of the taxa *Globigerina bulloides*, *G. ruber* (white and pink), *Globoturborotalita rubescens*, *Globigerinella siphonifera*, *Globigerinita glutinata*, *Globorotalia inflata* and *Orbulina universa*. Benthic foraminifers were recorded throughout the studied interval, except in the S1 layer, where only 3 sample host a poorly abundant and poorly diversified association composed by *Cassidulina laevigata*, *Cibicidoides pseudoungerianus* and *Cibicidoides kullenbergi*. Benthic foraminifer then reappears at 20 cm. The benthic foraminifers assemblage was dominated by *C. laevigata*, that is replaced by *Quinqueloculina akneriana* in a couple of sample at 55.5 cm and 35.5. Minor component of the assemblage are *C. kullenbergi* and *C. pseudoungerianus*; the remaining taxa were rare and scattered present.

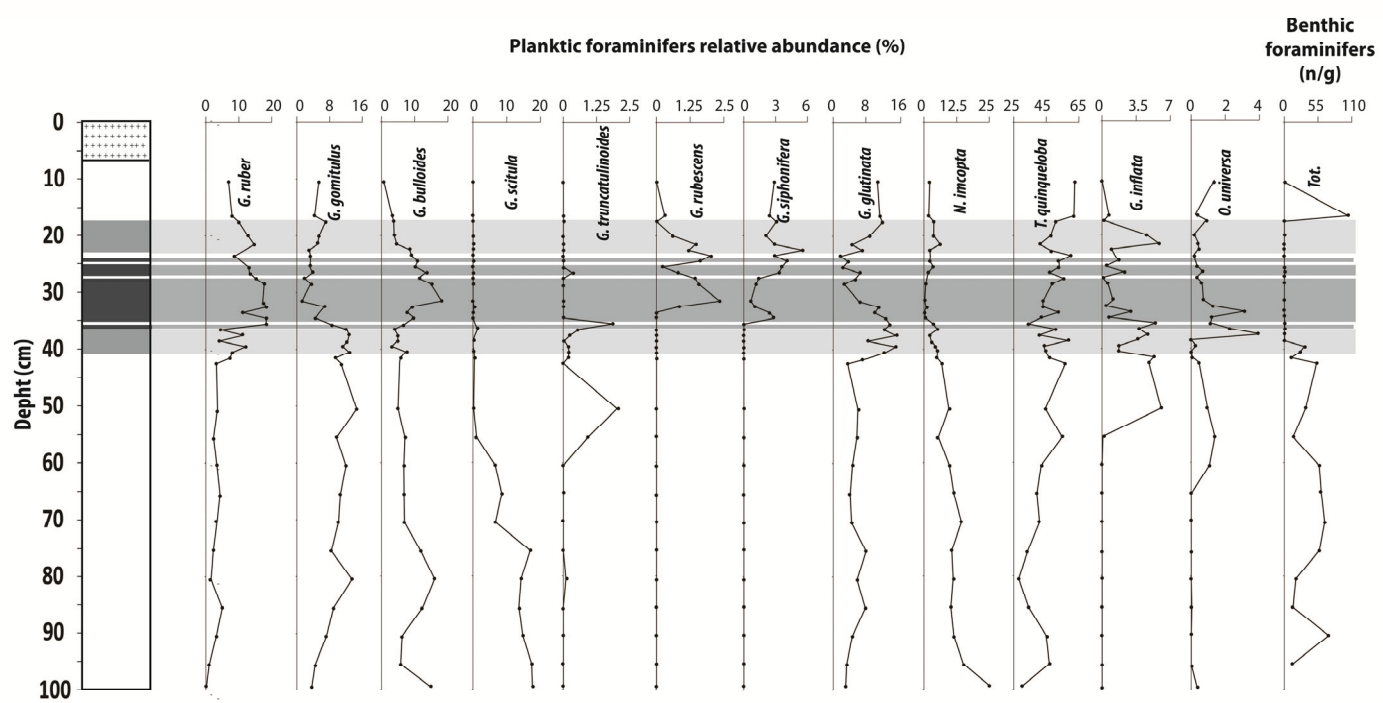


Figure S3: Planktic and benthic foraminiferal abundance.